Available online at www.sciencedirect.com
ScienceDirect
Journal of the European Ceramic Society 27 (2007) 2237–2243
www.elsevier.com/locate/jeurceramsoc

Thick-film PTC thermistors and LTCC structures: The dependence of the electrical and microstructural characteristics on the firing temperature

Marko Hrovat [a,*], Darko Belavič [b], Jaroslaw Kita [c], Janez Holc [a], Jena Cilenšek [a], Leszek Golonka [c], Andrzej Dziedzic [c]

[a] Jožef Stefan Institute, Jamova 39, 1000 Ljubljana, Slovenia
[b] HIPOT-R&D, d.o.o., Trubarjeva 7, 8310 Sentjernej, Slovenia
[c] Wroclaw University of Technology, Wybrzeze Wyspianskiego 27, 50-370 Wroclaw, Poland

Received 19 May 2006; received in revised form 28 July 2006; accepted 7 August 2006
Available online 27 September 2006

Abstract

The electrical and microstructural characteristics of 1 kΩ/sq thick-film thermistors with high positive temperature coefficients of resistivity, i.e., PTC 5093 (Du Pont) fired either on “green” LTCC (low-temperature co-fired ceramics) substrates or buried within LTCC structures, were evaluated. The thermistors were fired at different temperatures to study the influence of firing temperature on the electrical characteristics. The noise indices of the surface resistors fired at temperatures between 850 °C and 950 °C were very low, around −30 dB. The TCRs of the evaluated PTC thermistors were over 3000×10^{-6}/K. The dependence of the resistivity on the temperature between −25 °C and 125 °C was linear, with the values of R^2 being better than 0.9999, regardless of the processing conditions. These results show that PTC thermistors co-fired on LTCC substrates can be used for temperature sensors in MCM-Cs as well as in MEMS structures. However, when the thermistors were buried in the LTCC substrates, the LTCC structures delaminated during firing and blisters formed, leading to high sheet resistivities and high noise indices. This delamination is attributed to the different sintering rates of the PTC and LTCC materials as well as to the expansion of the air bubbles captured in the viscous glass of the PTC material.

Keywords: Films; Electron microscopy; Electrical properties; Sensors; LTCC

1. Introduction

Thick-film resistors are made by screen-printing thick-film paste onto insulating, mainly alumina, substrates. After printing and drying, the thick-film pastes are fired in a belt furnace. Thick-film resistor pastes consist basically of a conducting phase, a lead borosilicate-based glass phase and an organic vehicle. This organic material is burned out between 300 °C and 400 °C during the high-temperature processing. The ratio between the conductive and the glass phases roughly determines the specific resistivity of the resistor. In most modern resistor compositions the conductive phase is either RuO_2 or ruthenates, mainly bismuth or lead ruthenates.[1–5] During the firing cycle all the constituents of the resistor material react with each other. The main change during firing is the transition from a mixture of glass grains and, usually, much finer grains of the conductive phase in the thick-film paste, into conductive chains throughout the sintered glass in the fired resistor. The resistors, however, are only a relatively short time (typically 10 min) at the highest temperature (typically 850 °C). Because of this, the reactions between the constituents of the resistor material do not reach equilibrium, so that the characteristics of the fired materials are, in a way, a compromise as a consequence of this frozen non-equilibrium.[6–8]

The main requirements for “normal” thick-film resistors are long-term stability, relatively narrow tolerances of the sheet resistivities after firing, low noise indices and, in particular, low temperature coefficients of resistivity (TCR), which are, for most commercial resistor series, below 100×10^{-6}/K. However, for some temperature-sensing or temperature-compensating applications resistors with a large, positive and linear temperature dependence of resistivity are required. Thick-film thermistors

* Corresponding author. Tel.: +386 1 477 3900; fax: +386 1 426 3126.
E-mail address: marko.hrovat@ijs.si (M. Hrovat).

0955-2219/$ – see front matter © 2006 Elsevier Ltd. All rights reserved.
doi:10.1016/j.jeurceramsoc.2006.08.005

with positive TCRs (PTC) have a positive and linear temperature dependence of resistivity, as described by the following linear equation:

$$R(T) = R_0(1 + aT) \quad (1)$$

where R_0 (Ω) is the resistance at the reference temperature, T the temperature (K) and a is the TCR (1/K).

PTC thick-film resistors are prepared by "loading" a high concentration of RuO_2 into a glass phase. RuO_2 has a relatively low specific resistivity, $40 \times 10^{-6}\ \Omega$ cm, and a positive, linear, metallic-like resistivity versus temperature dependence, with a TCR of 7000×10^{-6}/K for single crystals and a few 1000×10^{-6}/K for sintered microcrystalline samples.[9,10] Due to the high concentration of RuO_2, the sheet resistivities are relatively low, between 1 Ω/sq and 10 Ω/sq. The majority of thick-film PTC thermistors are in this resistivity range.

The Du Pont 5093 PTC thermistors with a sheet resistivity of 1 kΩ/sq are currently the thermistors with the highest sheet resistivity values commercially available, to the best of the authors' knowledge. The high resistivity is achieved with materials that are not based on ruthenium oxide, but on ruthenates with an addition of copper oxide.[11,12] It is known that at high enough temperatures and/or long enough firing times the ruthenate conductive phase in most ruthenate-based thick-film resistors decomposes due to interactions with a glass phase into RuO_2 and, for example, PbO or Bi_2O_3 in the case of lead ruthenate or bismuth ruthenate, respectively.[8,13]

Because of the added copper oxide, the RuO_2, which is formed due to the decomposition of the ruthenate phase in the 5093 PTC thermistors during firing, crystallises in the form of needle-like grains, which produce the conducting network through the glass matrix. This is a result of a specific crystallographic relationship between the CuO and the RuO_2,[14] and is shown schematically in Fig. 1a. The microstructure of the 5093 thermistor fired for 10 min at 850 °C is shown in Fig. 1b.[15] The needle-like RuO_2 grains are denoted "R", and the $SiZrO_4$ particles are denoted "SZ".

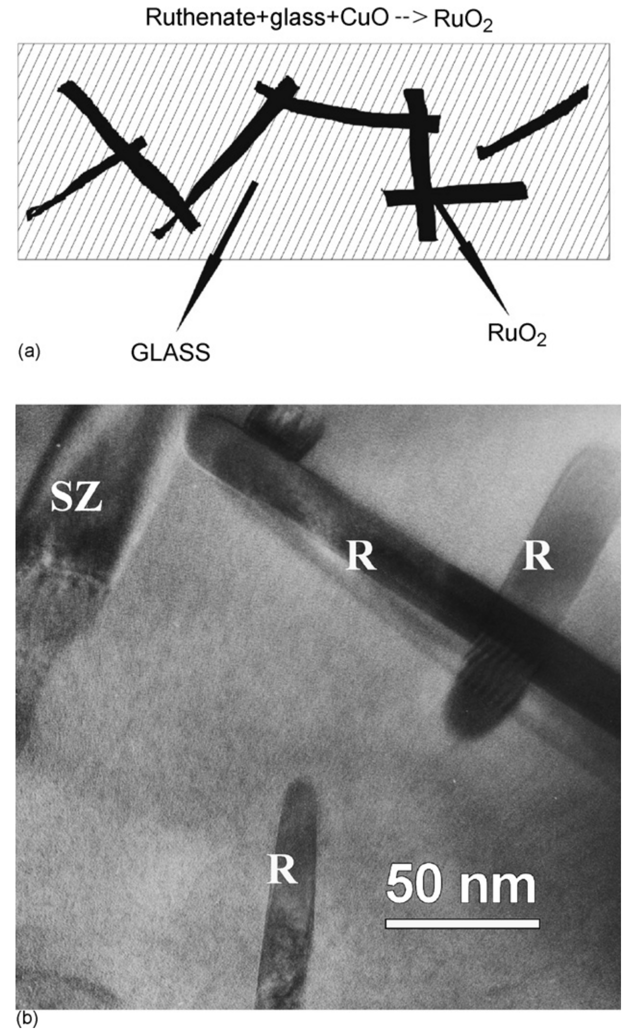

Fig. 1. (a) The ruthenate conductive phase in thick-film resistors decomposes due to interactions with a glass phase into RuO_2. Due to added copper oxide the RuO_2 crystallises in the form of needle-like grains. Schematically. (b) TEM micrograph of 5093 thermistor, fired for 10 min at 850 °C. Elongated RuO_2 particles are denoted "R" and $SiZrO_4$ particles are denoted "SZ".[15]

Ceramic multi-chip modules (MCM-Cs) are multilayer substrates with buried conductor lines, which means that they have a high density of interconnections. An additional advantage of the smaller size and higher density is the ability to integrate screen-printed resistors, or occasionally, capacitors and inductors. These screen-printed components can be placed either beneath the discrete components on the surface of the multilayer dielectric or buried within the multilayer structure. Low-temperature co-fired ceramic (LTCC) materials, which are sintered at the low temperatures typically used for thick-film processing, i.e., around 850 °C, are widely used for the production of MCM-Cs, especially for telecommunications and automotive applications. To sinter to a dense and non-porous structure at these, rather low, temperatures, it has to contain some low-melting-point glass phase. LTCCs are either based on crystallisable glass or a mixture of glass and ceramics; for example, alumina, silica or cordierite ($Mg_2Al_4Si_5O_{18}$).[16–20] The glass could presumably interact with, for example, thick-film resistors leading to changes in the electrical characteristics. Some of the results for the resistor/LTCC combinations and the influences on the electrical characteristics can be found in.[21–24]

Thick-film resistors with high TCRs are of interest as temperature sensors in MCM-Cs as well as in MEMS (Micro Electro Mechanical Systems).[25–28] The thick-film PTC thermistors were developed for firing on alumina substrates. Therefore, their compatibility and interactions with the rather glassy LTCC substrates, leading to changes in the electrical characteristics, need to be evaluated. The aim of this research was to study the characteristics of thick-film PTC 5093 thermistors fired either on or buried within Du Pont LTCC 951 substrates, and to obtain some understanding of the development of the thick-film thermistor's microstructural characteristics and electrical characteristics, i.e., sheet resistivity, beta factor and noise, during the firing process. The thermistors were fired at temperatures from 850 °C to 950 °C, and also for a relatively long time (3 h) at 950 °C to allow reactions to reach or at least to come close to equilibrium. The obtained results would be also usable for application were the

LTCC structures are fired at higher temperatures than standard 850 °C. The characteristics of PTC thermistors fired at different temperatures on alumina substrates[15] are used as a reference. The nominal TCR of the PTC 5093 is $2750 \pm 250 \times 10^{-6}$/K.

2. Experimental

The LTCC substrates were made by laminating three layers of LTCC tapes at 70 °C and at a pressure of 200 bar for the surface PTC thermistors. For the buried thermistors two layers were laminated. The conductive Ag/Pd tracks were printed and dried on the laminated LTCC substrates. After this the 5093 PTC thermistors were printed and dried. For the buried resistors, which were printed on the laminated two-layer substrates, the upper tape with the laser-cut openings (for the electrical measurements) was pressed into the two-layer structures and laminated again under the same conditions. The prepared samples were co-fired at maximum temperatures of 850 °C, 875 °C and 950 °C for 10 min, and at 950 °C for 3 h. The firing profiles also included a 1-h-long "pause" at 450 °C to burn-out the organic materials from the LTCC tapes. Cold (from −25 °C to 25 °C) and hot (from 25 °C to 125 °C) TCRs were calculated from resistivity measurements at −25 °C, 25 °C, and 125 °C. The current noise was measured in dB on 100-mW loaded resistors using the Quan Tech method (Quan Tech Model 315-C).

The dimensions of the resistor layers for the microstructural analysis and the X-ray diffraction (XRD) analysis, which were printed and fired without conductor terminations on the top of LTCC substrates, were 12.5 mm × 12.5 mm. For the microstructural investigation the samples were mounted in epoxy in a cross-sectional orientation and then cut and polished using standard metallographic techniques. A JEOL JSM 5800 scanning electron microscope (SEM) equipped with an energy-dispersive X-ray analyzer (EDS) was used for the overall microstructural and compositional analysis. Boron oxide, which is also present in the glass phase, cannot be detected in the EDS spectra because of the low relative boron weight fraction in the glass and the strong absorption of the boron Kα line during EDS analysis in the glass matrix. Dried thermistors (150 °C) and thermistors fired at 850 °C were analysed by X-ray diffraction (XRD) analysis with a Philips PW 1710 X-ray diffractometer using Cu Kα radiation.

For the sintering studies of the LTCC and PTC materials the organic phase of the LTCC tapes and the PTC paste was dissolved in acetone. The obtained powders were pressed into pellets with a diameter of 6 mm and a height of 3 mm. The dimensional changes were measured in a heating-stage microscope. The heating rate was 10 K/min.

3. Results and discussion

The X-ray diffraction spectra of the PTC 5093 thermistors dried at 150 °C, and co-fired for 10 min at 850 °C, 875 °C, 950 °C and 3 h at 950 °C on LTCC substrates are shown in Fig. 2. The spectrum of ruthenium oxide, denoted "RuO_2", is also included. The peaks of the ruthenate phase and the copper oxide in the dried films are denoted "Ru" and "Cu_2O", respectively. After

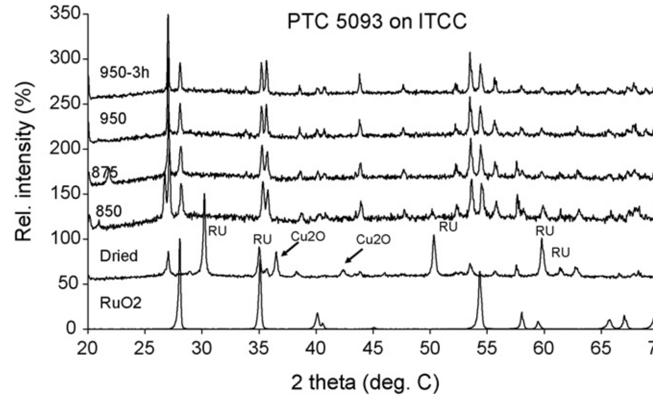

Fig. 2. The X-ray diffraction spectra of the PTC 5093 thermistors dried at 150 °C, and co-fired on the LTCC substrates for 10 min at 850 °C, 875 °C, 950 °C and 3 h at 950 °C on LTCC substrates The spectrum of ruthenium oxide, denoted "RuO_2", is also included. The peaks of the ruthenate phase and the copper oxide in the dried films are denoted "RU" and "Cu_2O", respectively.

firing the peaks of ruthenate and Cu_2O disappear and the peaks of RuO_2 appear. The decomposition of ruthenate and the formation of the RuO_2 during firing are due to the interaction between the glass phase and the ruthenate in the PTC 5093 thermistor (see Section 1).

Cross-sections of the PTC 5093 thermistors fired on LTCC substrates for 10 min at 850 °C and for 3 h at 950 °C are shown in Figs. 3 and 4, respectively. The LTCC substrate is on the right. After firing at 850 °C the PTC layer is densely sintered with small white and black inclusions. The EDS microanalysis of the light-coloured spots shows a high concentration of Ru and Cu, while the black inclusions are a silica-rich phase. The LTCC material is composed of a glassy matrix (grey phase) and an alumina filler (dark phase). After firing for 3 h at 950 °C the dark inclusions in the PTC layer disappear. In the reaction layer at the interface between the PTC and the LTCC elongated crystals rich in alumina and silica appear. The PbO-rich glass phase from the PTC film infiltrated the LTCC substrate to a depth of around 20 μm.

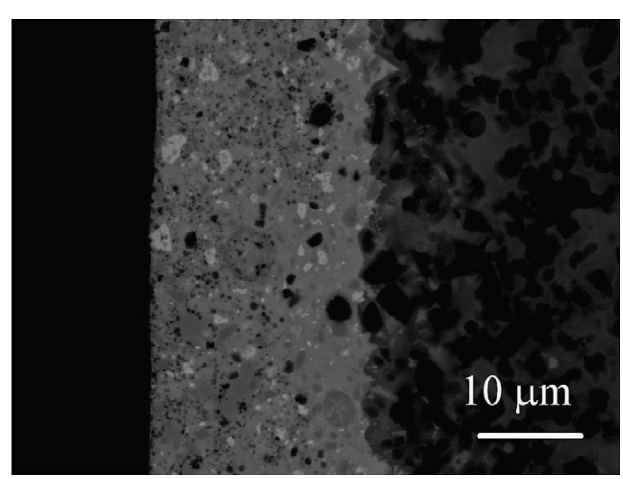

Fig. 3. Cross-section of the PTC 5093 thermistor, fired at 850 °C on LTCC. The LTCC substrate is on the right.

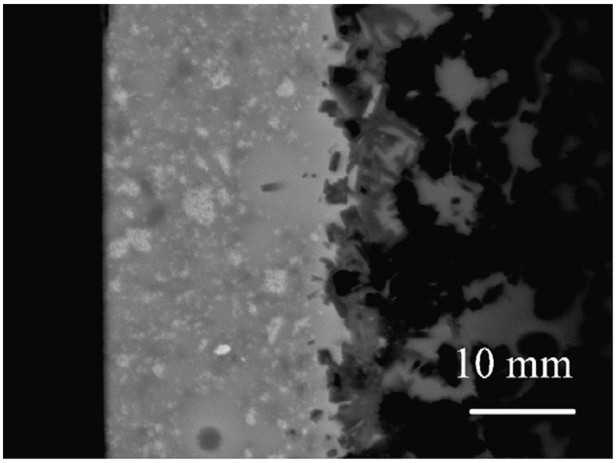

Fig. 4. Cross-section of the PTC 5093 thermistor, fired 3 h at 950 °C on LTCC. The LTCC substrate is on the right.

During the firing of the buried PTC thermistors the structures delaminated forming the cavities between the upper and lower LTCC tapes. This also resulted in the deformation of the LTCC tapes. The microstructure of the sample fired for 10 min at 850 °C is shown in Fig. 5a. The light layers on the inner surfaces of the cavity are PTC films. Some cracks appear at the PTC/LTCC interface and in the PTC film. The microstructure

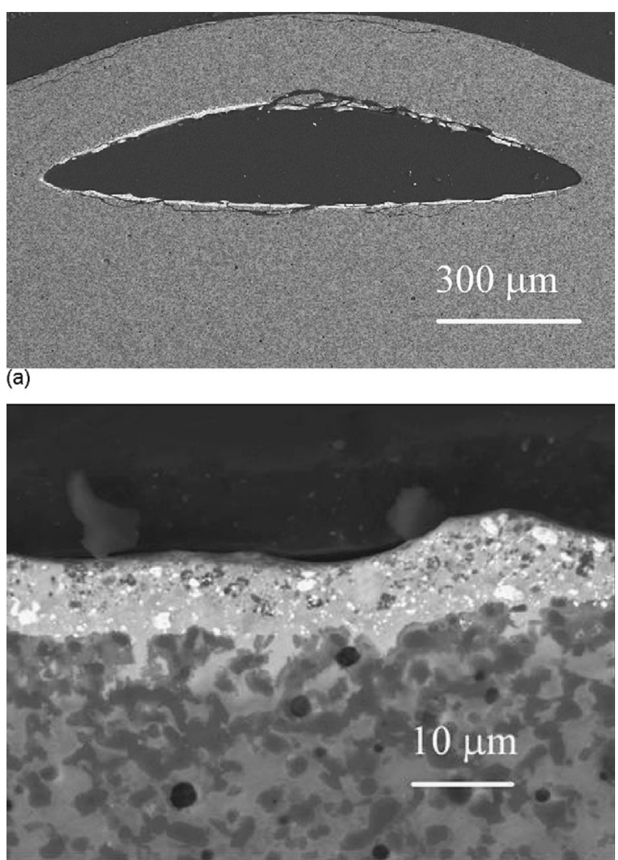

Fig. 5. (a) Cross-section of buried PTC 5093 thermistor, fired at 850 °C. The structure delaminated during firing. (b) Microstructure of buried PTC 5093 thermistor, fired at 850 °C. Higher magnification.

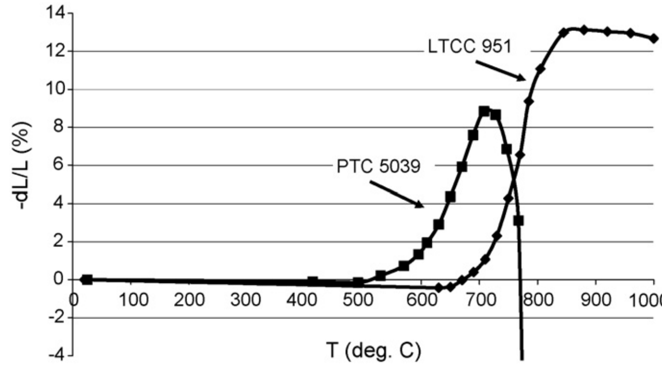

Fig. 6. Sintering curves of the LTCC 951 and PTC 5093 materials.

of the PTC film shown at higher magnification in Fig. 5b is similar to the microstructures of the films fired on the top of the LTCC substrates. However, the thickness of the buried PTC film is around half that of the thickness of the films on the LTCC because the single layer separated into two layers on the bottom and the top of the cavity.

The EDS analysis of the PTC layers fired on the top of the LTCC and buried within the LTCC tapes, fired for 10 min at 850 °C and 3 h at 950 °C, showed that the concentrations of most of the analysed elements are similar in all the samples. The main exception is the concentration of alumina. The concentration of Al_2O_3 for the samples fired for 3 h at 950 °C is nearly three times higher (8 mol% versus 3 mol%) than in the samples fired for 10 min at 850 °C. This indicates the diffusion of Al_2O_3 from the LTCC into the PTC takes place at higher temperatures and during longer firing times.

The sintering curves of the LTCC and the PTC materials are shown in Fig. 6. A possible explanation for the blistering of the samples with buried PTC thermistors is as follows. The LTCC starts to sinter at around 650 °C. The final shrinkage is 13% at 850 °C. The PTC powder starts to sinter at a temperature that is approximately 100 K lower. The sample contracts by 9% at 700 °C and then starts to expand with increasing temperature. The microstructure of the PTC pellet that was heated to 780 °C in

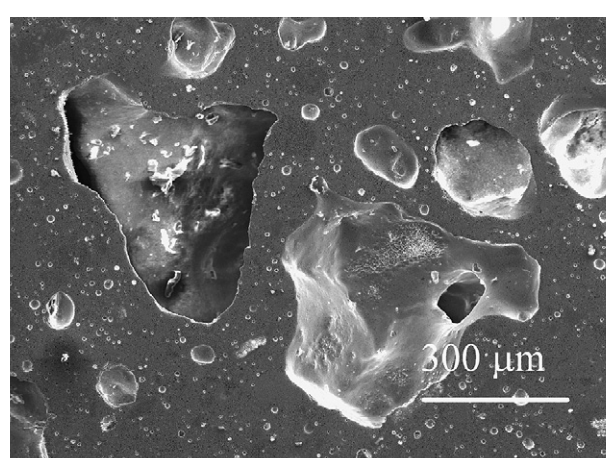

Fig. 7. The microstructure of the PTC material heated to 780 °C in the heating-stage microscope.

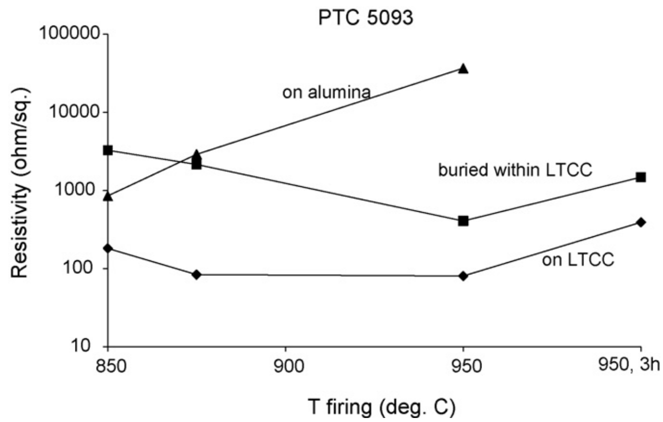

Fig. 8. The logarithm of sheet resistivities vs. firing temperatures for PTC 5093 thermistors co-fired either on or buried within LTCC structures. Results for thermistors fired on alumina substrates[15] are added.

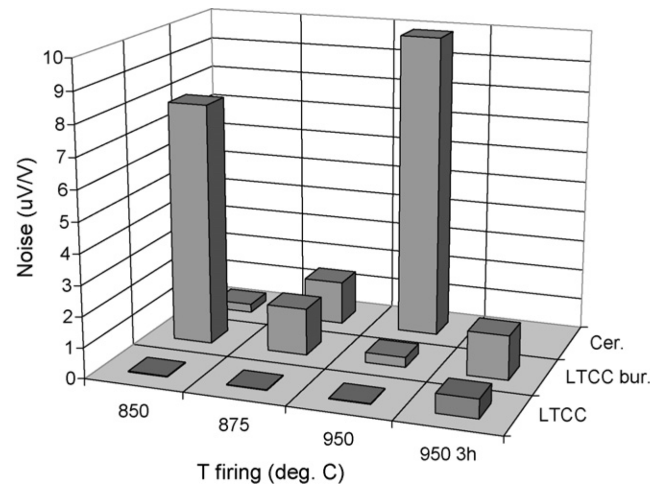

Fig. 9. The noise indices vs. firing temperatures for PTC 5093 thermistors co-fired either on or buried within LTCC structures. Results for thermistors fired on alumina substrates[15] are added.

the heating-stage microscope is shown in Fig. 7. The microstructure shows sintered PTC material with entrapped pores up to half a millimetre in size. The pores were formed when the air was captured in a viscous glass phase. Different shrinkage rates – as mention before, the PTC starts to sinter at a temperature that is approximately 100 K lower – led to delamination of the LTCC structures. At temperatures over 720 °C the glass in the PTC material softens and starts to expand, presumably due to the air trapped in the pores. The glass phase also adheres to the lower and upper LTCC tapes. The entrapped air expands with the increasing temperature and inflates the cavity that was probably formed during the early stage of PTC and LTCC sintering due to delamination. At 780 °C the LTCC material is densely sintered and is, therefore, an additional barrier for the air trapped in the cavity.

The sheet resistivities, the cold (−25 °C to 2 °C) and hot (25 °C to 125 °C) TCRs, and the noise indices of the PTC 5093 thick-film thermistors fired for 10 min at 850 °C, 875 °C, 950 °C and 3 h at 950 °C either on the surface or buried within LTCC substrates are shown in Table 1. The results for the thermistors fired on alumina substrates[15] are added. The sheet resistivities and noise indices versus firing temperatures are shown in Figs. 8 and 9, respectively. In Fig. 9 the thermistors, fired on the surface or buried within the LTCC structures and fired on alumina substrates, are denoted “LTCC”, LTCC bur. and “Cer.”, respectively. Note that the noise indices are shown in “dB” in Table 1 and in “uV/V” in Fig. 4. These two units are related by the simple equation:

$$\text{noise (dB)} = 20 \times \log \text{noise} \left(\frac{\text{uV}}{\text{V}}\right)$$

The sheet resistivities of the PTC thermistors fired at 850 °C on LTCC substrates are lower than the nominal resistivity of 1 kΩ/sq. At the same firing temperature the resistivities of the buried thermistors are around one order of magnitude higher than the thermistors co-fired on top of the LTCC. They also have higher noise indices. These results are a consequence of the delamination cracks observed in the microstructure (Fig. 5a). The TCR values of the surface resistors are higher than 3000×10^{-6}/K, with the exception of the films fired for

Table 1
Sheet resistivities, cold (−25 °C to 2 °C) and hot (25 °C to 125 °C) TCRs, noise indices of the PTC 5093 thick-film thermistors fired for 10 min at 850 °C, 875 °C, 950 °C and 3 h at 950 °C either on the surface or buried within LTCC substrates

T firing (°C)	Substrate	*R* sheet (kΩ/sq)	Cold TCR ($\times 10^{-6}$/K)	Hot TCR ($\times 10^{-6}$/K)	Noise (dB)
850	LTCC surface	0.18	3075	3055	−32
	LTCC buried	3.27	2380	2355	18
	Al_2O_3 [15]	0.85	2540	2560	−11
875	LTCC surface	0.08	3240	3250	−33
	LTCC buried	2.15	2450	2430	3.7
	Al_2O_3 [15]	2.9	2380	2400	3.0
950	LTCC surface	0.08	3260	3240	−32
	LTCC buried	0.41	2400	2350	−10
	Al_2O_3 [15]	37	2300	2350	20
950, 3 h	LTCC surface	0.4	2320	2380	−4.2
	LTCC buried	1.5	1490	1450	3.2
	Al_2O_3 [15]	/[a]	/	/	/+

[a] Resistivities too high to measure.

3 h at 950 °C. The TCRs of the buried resistors are comparable with the values obtained on alumina substrates, i.e., around 2400×10^{-6}/K. However, note that the resistivity versus temperature dependences are in all cases remarkably linear, with the values of R^2 being better than 0.9999, regardless of the processing conditions. The noise indices of the PTC thermistors co-fired on the surface of the LTCC ceramics are lower than the values on the alumina substrates and also lower than those of the buried thermistors. The differences in the electrical characteristics of the PTC thermistors fired on the LTCC substrates compared with the results on the alumina substrates can be attributed to the interaction between the PTC films and the glassy LTCC substrates during firing.

4. Conclusions

Because the thick-film thermistors with a high positive TCR were developed for firing on inert alumina substrates their compatibility with (rather glassy) LTCC substrates was evaluated. The PTC 5093 thermistors with high sheet resistivities (1 kΩ/sq) were printed and co-fired either on the surface of the LTCC substrates or buried within the LTCC structures. The thermistors were fired at temperatures from 850 °C to 950 °C, and also for a relatively long time (3 h) at 950 °C to study the influence of firing temperature on the electrical characteristics. The results showed that the buried resistors co-fired in the LTCC structures cannot be used for practical applications. During firing, blisters formed and the LTCC tapes mechanically deformed.

The sheet resistivities of the PTC 5093 thermistors co-fired on LTCC are lower than for samples prepared on alumina. The noise indices of the surface resistors fired at temperatures between 850 °C and 950 °C are very low, around −30 dB. The TCRs of the thermistors are over 3000×10^{-6}/K. The dependence of resistivity versus temperature between −25 °C and 125 °C is linear, with the values of R^2 being better than 0.9999, regardless of the processing conditions. These results suggest that PTC thermistors co-fired on LTCC substrates could be used for a very precise temperature sensor in MCM-Cs as well as in MEMS structures.

Acknowledgements

The authors wish to thank Mr. Mitja Jerlah (HIPOT-R&D) for printing and firing the samples as well as for measuring the electrical characteristics. The financial support of the Slovenian Research Agency is gratefully acknowledged.

References

1. Vest, R. W., Materials science of thick film technology. *Ceram. Bull.*, 1986, **65**(4), 631–636.
2. Inokuma, T. and Taketa, Y., Control of electrical properties of RuO_2 thick film resistors. *Active Passive Elect. Comp.*, 1987, **12**(3), 155–166.
3. Abe, O., Taketa, Y. and Haradome, M., The effect of various factors on the resistivity and TCR of RuO_2 thick film resistors – relation between the electrical properties and particle size of constituents, the physical properties of glass and firing temperature. *Active Passive Elect. Comp.*, 1988, **13**(2), 76–83.
4. Crosbie, G. M., Johnson, F. and Trela, W., Processing factor dependence of resistivity parameters of ruthenate-based thick film resistors with low temperature coefficients. *J. Appl. Phys.*, 1998, **84**(5), 2913–2919.
5. Hrovat, M., Belavič, D., Samardžija, Z. and Holc, J., A characterisation of thick film resistors for strain gauge applications. *J. Mater. Sci.*, 2001, **36**(11), 2679–2689.
6. Yamaguchi, T. and Kato, S., Evaluation of commercial 96% alumina substrates and mechanism of paste-substrate interaction. *Ceram. Trans.*, 1990, **15**, 575–582.
7. Morten, B., Masoero, A., Prudenziati, M. and Manfredini, T., Evolution of ruthenate-based thick film cermet resistors. *J. Phys. D: Appl. Phys.*, 1994, **27**(10), 2227–2235.
8. Hrovat, M., Benčan, A., Belavič, D., Holc, J. and Dražič, G., The influence of firing temperatures on the electrical and microstructural characteristics of thick film resistors for strain gauge applications. *Sens. Actuators A*, 2003, **103**, 341–352.
9. van Loan, P. R., Conductive ternary oxides of ruthenium, and their use in thick film resistor glazes. *Ceram. Bull.*, 1972, **51**(3). pp. 231–233, 242.
10. Pierce, J. W., Kuty, D. W. and Larry, J. R., The chemistry and stability of ruthenium based resistors. *Solid State Technol.*, 1982, **25**(10), 85–93.
11. Hormadaly, J., Thermistor composition, US Patent 4,906,406, March 6, 1990.
12. Hormadaly, J., Thermistor composition, US Patent 4,961,999, October 9, 1990.
13. Hrovat, M., Samardžija, Z., Holc, J. and Belavič, D., Microstructural and electrical characteristics of some "overfired" thick-film resistors. *J. Mater. Sci. Lett.*, 2001, **20**(4), 347–351.
14. Jiang, J. C., Crosbie, G. M., Tian, W., Cameron, K. K. and Pan, X. Q., Transmission electron microscopy structure and platinum-like temperature coefficient of resistance in ruthenate-based thick film resistor with copper oxide. *J. Appl. Phys.*, 2000, **88**(2), 1124–1128.
15. Hrovat, M., Belavič, D., Benčan, A., Holc, J. and Dražič, G., A characterization of thick-film PTC resistors. *Sens. Actuators A*, 2005, **117**(2), 256–266.
16. Jean, J.-H. and Chang, C.-R., Camber development during cofiring Ag-based low-dielectric-constant ceramic package. *J. Mater. Res.*, 1997, **12**(10), 2743–2750.
17. Doty, R. E. and Vajo, J. J., A study of field-assisted silver migration in low temperature cofirable ceramic. In *Proceedings of the 1995 International Symposium on Microelectronics ISHM-95*, 1995, pp. 468–474.
18. Ting, C.-J., Hsi, C.-S. and Lu, H.-J., Interactions between ruthenium-based resistors and cordierite-glass substrates in low temperature co-fired ceramics. *J. Am. Ceram. Soc.*, 2000, **83**(12), 23945–32953.
19. Jones, W. K., Liu, Y., Larsen, B., Wang, P. and Zampino, M., Chemical, structural and mechanical properties of the LTCC tapes. In *Proceedings of the 2000 International Symposium on Microelectronics IMAPS-2000*, 2002, pp. 669–674.
20. Mohanram, A., Messing, G. L. and Green, D. J., Densification and sintering viscosity of low-temperature co-fired ceramics. *J. Am. Ceram. Soc.*, 2005, **88**(10), 2681–2689.
21. Rodrigues, M. A., Yang, P., Kotula, P. and Dimos, D., Microstructure and phase development of buried resistors in low temperature co-fired ceramics. *J. Electroceram.*, 2000, **5**(3), 217–223.
22. Dziedzic, A., Golonka, L. J., Kita, J., Thust, H., Drue, K.-H., Bauer, R. *et al.*, Electrical and stability properties and ultrasonic microscope characterization of low temperature co-fired ceramics resistors. *Microelectron. Reliab.*, 2001, **41**, 669–676.
23. Yang, P., Rodrigues, M. A., Kotula, P., Miera, B. K. and Dimos, D., Processing, microstructure, and electric properties of buried resistors in low-temperature co-fired ceramics. *J. Appl. Phys.*, 2001, **89**(7), 4175–4182.

24. His, C.-S., Chen, D.-F., Shieh, F.-M. and Fu, S.-L., Processing of LTCC with embedded RuO_2-based resistors. *Mater. Chem. Phys.*, 2002, **78**, 67–72.
25. Dziedzic, A. and Golonka, L. J., Thick-film and LTCC thermistors. In *Proceedings of the XXIV International Conference IMAPS, Poland 2000*, ed. W. Zaraska, A. Cichocki and D. Szwagierezak, 2000, pp. 77–83.
26. Zhong, J. and Bau, H. H., Thick film thermistors printed on LTCC tapes. *Am. Ceram. Bull.*, 2001, **80**(10), 39–42.
27. Birol, H., Maeder, T., Jacq, C. and Ryser, P., Effect of firing conditions on thick-film PTC thermistor characteristics in TLCC technology. In *Proceedings of the IMAPS Ceramic Interconnect Technology Conference*, 2004, pp. 106–109.
28. Birol, H., Maeder, T., Jacq, C. and Ryser, P., Investigation of interactions between co-fired LTCC components. *J. Eur. Ceram. Soc.*, 2005, **25**(12), 2065–2069.